

## Mixed Anatase/Rutile Phase of Ag Doped TiO<sub>2</sub> Film for Dye Degradation

Noor Kamalia Abd Hamed<sup>1</sup>, Mohd Khairul Ahmad<sup>1\*</sup>, Paul Terence Santana<sup>1</sup>, Nafarizal Nayan<sup>1</sup>, Mohd Hazli Mazlan<sup>1</sup>, Soon Chin Fhong<sup>1</sup>, Mohd Hafiz Mamat<sup>2</sup>, Suriani Abu Bakar<sup>3</sup> and Shimomura Masaru<sup>4</sup>

<sup>1</sup>Microelectronic and Nanotechnology Shamsuddin Research Centre (MiNT-SRC), Faculty of Electrical and Electronic Engineering, Universiti Tun Hussein Onn Malaysia, 86400 Parit Raja, Batu Pahat, Johor, Malaysia  
mel\_leya@yahoo.com, akhairul@uthm.edu.my

<sup>2</sup>Nano-Electronic Centre, Faculty of Electrical Engineering, Universiti Teknologi Mara, 40450 Shah Alam, Selangor, Malaysia

<sup>3</sup>Nanotechnology Research Centre, Department of Physic, Faculty of Science and Mathematics, Universiti Pendidikan Sultan Idris, 35900 Tanjung Malim, Perak, Malaysia

<sup>4</sup>Department of Engineering, Graduate School of Integrated Science and Technology, Shizuoka University, 432-8011 Hamamatsu, Shizuoka, Japan

### ABSTRACT

Mixed anatase/rutile Ag doped titanium dioxide (TiO<sub>2</sub>) film successfully fabricated with two simple step. Firstly, Ag doped rutile phase TiO<sub>2</sub> was fabricated by hydrothermal method at low temperature of 150°C for 10 hours and followed by various duration of immersion in taylor 320 solution for anatase phase. The various duration of immersion was studied to investigate the optimum time immersion to decorate anatase phase on Ag doped rutile phased TiO<sub>2</sub> film in assisting photocatalytic activity. The prepared samples were analyzed for their crystalline structure, morphology, composition, and photocatalytic activity using various analytical techniques such as X-ray diffraction (XRD), field emission scanning electron microscopy (FESEM), energy dispersive spectroscopy (EDX) and methylene blue (MB) degradation. It was observed that mixed phased of Ag doped TiO<sub>2</sub> film shows an excellent photocatalytic activity compared with the single phase. The optimum immersion time is 1 hour. The photodegradation of 1 hour immersion film was reached 100 percent degradation only for 90 minutes and increased up to 19% compared with no anatase phase film. It was proved that mixed phases has better degradation compared with single phase. The anatase phase helps to avoid recombination between electron and holes pair by capturing the electron and enhanced the photocatalytic activity since the anatase decorated on smooth surface of the rod which is no active area for photocatalytic activity.

**Key words:** Ag doped, anatase, methylene blue, photocatalytic, rutile, TiO<sub>2</sub>

### 1. INTRODUCTION

Environmental pollution become a serious problem originating from toxic organic pollutants in waste water that can harm the living organism. Releasing the toxic organic pollutant into various water bodies could abolish a fresh water resource. Therefore, an effective waste water treatment is desirable to save our environment for future generations. Generally, the conventional treatment of waste water were by flocculation, chemical oxidation, biological process, coagulation, membrane filtration and advanced oxidation process (AOP) [1], [2]–[4].

TiO<sub>2</sub> is one of the promising semiconductor that shows a great ability in AOP treatment [5]. Titanium dioxide (TiO<sub>2</sub>) has been investigate since discovered by Fujishima and Honda in 1971 for water splitting [6]. The increasing of environmental problem in society urge the researcher to optimized the ability of TiO<sub>2</sub> photocatalyst in environmental purification. Several advantages of TiO<sub>2</sub> are chemical stability, low cost, reusability and chemical inertness [7]–[9]. These advantages make TiO<sub>2</sub> a multifunctional material that can be used in various fields such as dye-sensitised solar cell (DSSC) [10], gas sensor [11], water splitting [12], hydrogen generation [13], and self-cleaning [14]. Among TiO<sub>2</sub> nanostructures, TiO<sub>2</sub> nanoflowers gives high surface area and high porosity [15]. Due to its high surface area, TiO<sub>2</sub> nanoflowers were used in application which it gives better response. Several drawbacks of TiO<sub>2</sub> that limit the photocatalytic property such as wide band gap. The band gap of anatase phase (3.2 eV) and rutile (3 eV) has a wide gap that electron must have to excite from valence band to conduction band [16]–[18]. In addition, TiO<sub>2</sub> also has high recombination between electron and hole pairs [19]. Mixed phase between anatase and rutile shows the

synergistic effect for enhanced photocatalytic activity. Several studies has been done into the development of the mix phases between rutile and anatase in charge separation between electron and holes pair [20]. These drawbacks also can be counter with the doping process with metal, non-metal and transition metal [21], [22]. The incorporation of nobel metal such as Au, Al and Ag into the parent lattice of TiO<sub>2</sub> may overcome the drawbacks of the photogenerated electron lifetime [23]. This metal will act as electron trapped that can give a longer lifetime to the electron that can react with the target contaminants [24]. This may due to the location of Ag Fermi level lower than TiO<sub>2</sub> conduction band [25]–[27]. Ag particle also has the ability to generate surface plasmon resonance (SPR) that can lower the band gap energy and subsequently enhance the photocatalytic activity of the film [28]. Ag exhibit a great ability in anti-bacterial effect which is a huge advantages for waste water treatment [29]. The synergistic effect of anatase/rutile heterojunction with Ag as electron trapper leads to excellent photocatalytic activity. Generally, many preparations have been reported in metal doped fabrication such as sol-gel spin coating [30], [31], solvothermal method [32], [33], electro-chemical synthesis [23] and reduction by using UV irradiation [34]. Though, the above-mentioned methods have several disadvantages of insufficient contact, low efficiency and consume a long period to prepare the sample.

From the previous study, most of the researcher mainly concentrated in synthesizing TiO<sub>2</sub> powders due to the higher photocatalytic activity than immobilized catalyst or film [35]. However, the disadvantages of post-separation between treated water and powder after the photocatalytic process can cause more serious problem to the aquatic life. Moreover, powder catalyst also has a limit in continues flow system [36]–[38]. Preparation of the catalyst on a film or immobilized catalyst may possible to overcome the stated problem.

In this project, mixed anatase/rutile phase of Ag doped TiO<sub>2</sub> film will be prepared using two simple step which is hydrothermal process and immersion in tayca 320. Hydrothermal technique could be a liquid-deposit method exploitation soft chemistry and provides a uniform thin film assisted with stable temperature and pressure. This film is expected to solve the stated problem and enhanced the photocatalytic activity. The administration of the experiment was done with tayca 320 for differential duration immersion of various hours shows the degradation level of the dye in waste water treatment increased compared by without the assisting of anatase phase. The fabricated TiO<sub>2</sub> were characterized by the exploitation of XRD, EDX, FESEM, and photodegradation of MB to investigate the morphology, elemental structural and efficiency of the film in photodegradation.

## 2. MATERIALS AND METHODS

### 2.1 Fabrication of mixed phases AR-Ag/TiO<sub>2</sub> film

Fluorine doped tin oxide (FTO) substrate was used in this experiments. The FTO glass was cut into 35 mm x 35 mm dimension. The substrate was cleaned using sonication method by using acetone, ethanol and deionized (DI) water with the volume ratios of (1:1:1) for 10 minutes followed by drying in ambient air. First stage of fabrication was by using hydrothermal method to fabricate rutile phase of Ag/TiO<sub>2</sub> film. 80 ml DI water was mixed with 80 ml of HCl. The solution was stirred for 5 minutes. The hot plate was set to 212°C. Then, put 0.0569 g of AgNO<sub>3</sub> and continued stirring for 30 minutes. The temperature was reduced to room temperature and 0.1 M of TBOT was dropped wisely into the solution. Stirred the solution until the solution is cleared. Put the FTO substrate with conducting FTO surface facing upward and pour the prepared solution into the Teflon made liner. Place the autoclave inside the oven at 150 °C for 10 hours. The autoclave was taken out from the oven and cooled down at room temperature. The prepared sample was rinse with DI water several time and dried at 100°C for 30 minutes. The second step was prepared for the addition of anatase phased. The immersion duration of rutile phase of Ag/TiO<sub>2</sub> film in tayca 320 was varied for 1 hour and 2 h ours. After immersion the sample was annealed at 450°C for 1 hours. R-Ag/TiO<sub>2</sub> denoted as rutile phase of Ag/TiO<sub>2</sub> film without anatase phase. AR1-Ag/TiO<sub>2</sub> denoted as mixed phases of anatase and rutile that immersed for 1 hour in tayca 320 while AR2-Ag/TiO<sub>2</sub> denoted as 2 hour immersion.

### 2.2 Characterization mixed phases AR-Ag/TiO<sub>2</sub> film samples

The successful fabricated mixed phases AR-Ag/TiO<sub>2</sub> film from the hydrothermal method and immersion method is characterized by using FESEM JEOL-7600F to study the surface morphologies and the elemental property of the samples. The XRD PANalytical X-Pert Powder was used to examine the structural property. The result shows the x-ray intensity versus 2θ. The range of the 2θ value was set from 20 to 80 degree. The efficiency of prepared sample was tested by using photodegradation of MB. The concentration of MB after treatment was examine by using UV-Vis spectroscopy.

### 2.3 Photocatalytic degradation of MB

Photocatalytic experiments was conducted to investigate the ability of AR-Ag/TiO<sub>2</sub> film in dye degradation. MB was used as a model of a waste water. 5 PPM concentration of MB with pH 12 was used in this study. The film was exposed with Xenon lamp (150 watt) to eliminate the unwanted impurity on top of the sample for 30 minutes. Then, the sample was

immersed in 100 ml of MB solution in dark condition for 30 minutes to promote adsorption-desorption of the sample. Then, the sample was irradiated with light for 120 minutes. The whole reactor was covered in a black box to refrain it from other source of light. Figure 1 shows the illustration of photocatalytic reactor for this study.

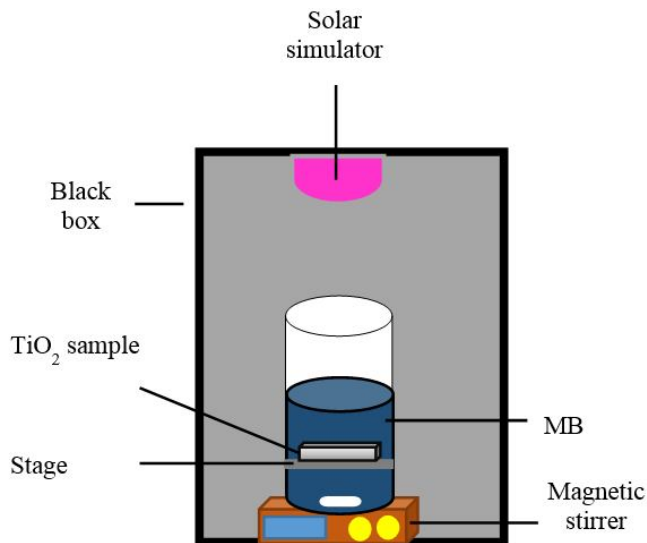


**Figure 1:** The illustration of photocatalytic reactor

At constant time interval, 3 ml of MB solution was withdrawn for sampling. The concentration of MB was observed at wavelength 664 nm. The percentage dye degradation was calculated by using Equation (1):

$$\text{MB degradation} = \frac{A_0 - A_t}{A_0} \times 100 \quad (1)$$

Where  $A_0$  is the initial absorbance of MB solution and  $A_t$  is the absorbance of MB solution at time  $t$ .

### 3. RESULTS AND DISCUSSIONS

#### 3.1 Structural property

The X-Ray Diffraction (XRD) characterization was used to study the structural properties of the  $\text{TiO}_2$  samples. The XRD pattern shown in Figure 2 shows the  $\text{TiO}_2$  were well crystallized. The peaks in XRD pattern shows anatase peak at 2 theta value of  $25.28^\circ$  on plane (101) and rutile peaks at  $27.45^\circ$ ,  $36.08^\circ$ ,  $41.23^\circ$ ,  $36.08^\circ$  and are related to R(110), R(101), R(111) and R(211) planes [39]. No anatase peak was detected for R-Ag/ $\text{TiO}_2$  sample. This may due to the acidic solution from the prepared sample that produce rutile phase. The acidic solution tend to produce rutile phase while alkaline solution tend to produce anatase phase in hydrothermal method [40]. The presence for anatase peak and rutile peaks can be viewed in the XRD spectra for both sample for AR1-Ag/ $\text{TiO}_2$  and AR2-Ag/ $\text{TiO}_2$ . The anatase peaks was

achieved by immersion with tayca 320 solution for each sample with time parameter of increment of 1 hour and 2 hours. Good crystallinity of catalyst will provide high electron mobility to the surface and enhanced the photocatalytic activity [41]. The role of anatase phase will explained in photodegradation of MB section. No Ag peak detected due to the lower percentage used and XRD unable to detect by XRD detector [27].

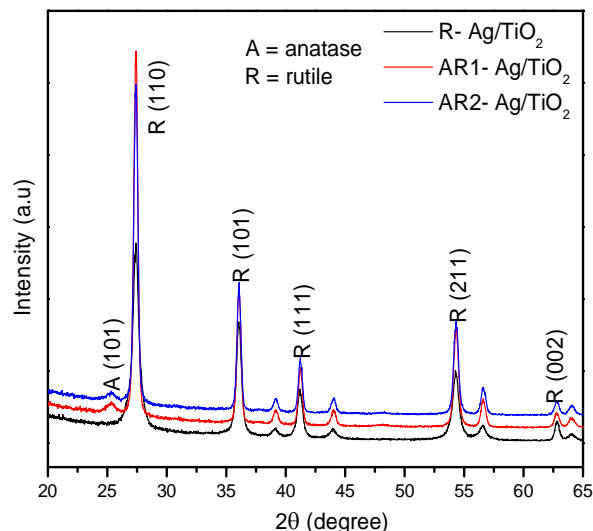


**Figure 2:** XRD pattern of R-Ag/ $\text{TiO}_2$  film and AR-Ag/ $\text{TiO}_2$  film prepared at 1 hour and 2 hours

#### 3.2 Elemental analysis

Elemental analysis was conducted by using EDX to investigate the elemental property of the prepared sample. Figure 3 shows the area that chosen for analysis and the element that exist in the sample. All the sample has a titanium (Ti) and oxygen (O). No impurity detected on the sample proved that our sample has pure  $\text{TiO}_2$  film. Table 1 shows the atomic percentage for prepared sample detected by EDX signal. The present of carbon (c) element may due to the carbon tape used during characterization of the sample. The R-Ag/ $\text{TiO}_2$  sample shows Ti and O as 22.58% and 74.69 %, respectively. For AR1-Ag/ $\text{TiO}_2$  sample shows Ti and O as 20.05 % and 76.62% while AR2-Ag/ $\text{TiO}_2$  sample shows Ti and O as 23.46 % and 74.24 %. No significant different between the samples. The obtained atomic percentage for all sample which confirms the stoichiometry of  $\text{TiO}_2$  elements.

**Table 1:** Atomic percentage of different sample

Element	R-Ag/TiO	AR1-Ag/TiO	AR2-Ag/TiO
t	2	2	2
	(%)	(%)	(%)
Ti	<b>22.58</b>	<b>20.05</b>	<b>23.46</b>
O	<b>74.69</b>	<b>76.62</b>	<b>74.24</b>
C	<b>2.73</b>	<b>3.33</b>	<b>2.30</b>

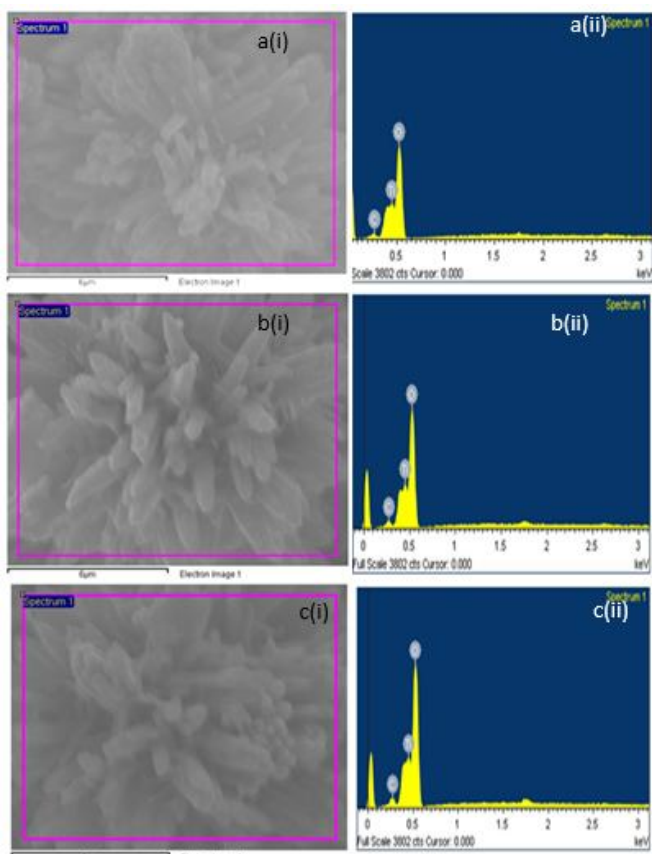


**Figure 3:** Elemental property of (a) R-Ag/TiO<sub>2</sub> film and AR-Ag/TiO<sub>2</sub> film prepared at (b) 1 hour and (c) 2 hours

### 3.3 Surface morphology

The field emission scanning electron microscopy (FESEM) is used to observe a surface morphology of the prepared sample. The FESEM has higher resolution, so that samples can be magnified at higher level. The surface morphology of the prepared TiO<sub>2</sub> film with different immersion hour duration are shown in Figure 4. It is indicated from figure 2(a) is without immersion while figure 4(b) has an hour of immersion and figure 4(c) has 2 hours immersion.

The rutile structure was formed from the chain of TiO<sub>6</sub> octahedral along the c-axis. The TiO<sub>6</sub> octahedral formed through one shared edge while two chain formed through points [42]. This may due to the Cl<sup>-</sup> ions restricted hydrolysis of titanium and form the rods structure instead of particle [43]. Detail information about formation of flower-like structure was explained in detail elsewhere [44]. All the films shows a flowerlike structure. The size of the rod is range 90 to 120 nm. No changes on morphology was expected after the immersion process. There is a layer build up on the flowerlike structure as the rate of immersion increases. This may due to the tayca 320 is absorbed and attach on the flower of TiO<sub>2</sub>. The inset images in each images shows the tayca 320 was successfully attach on the flower TiO<sub>2</sub>. The anatase nanoparticle with size 3-5 nm has

decorated on the smooth surface of rods of flower and hence enhanced the active site for photocatalytic process to take place. The rod structure has an exhibit good electron mobility and efficient electron and hole separation over TiO<sub>2</sub> surface[45], [46]. In addition, flower-structure can produce multiple reflection that provide more photon for TiO<sub>2</sub> to generate electron [47].

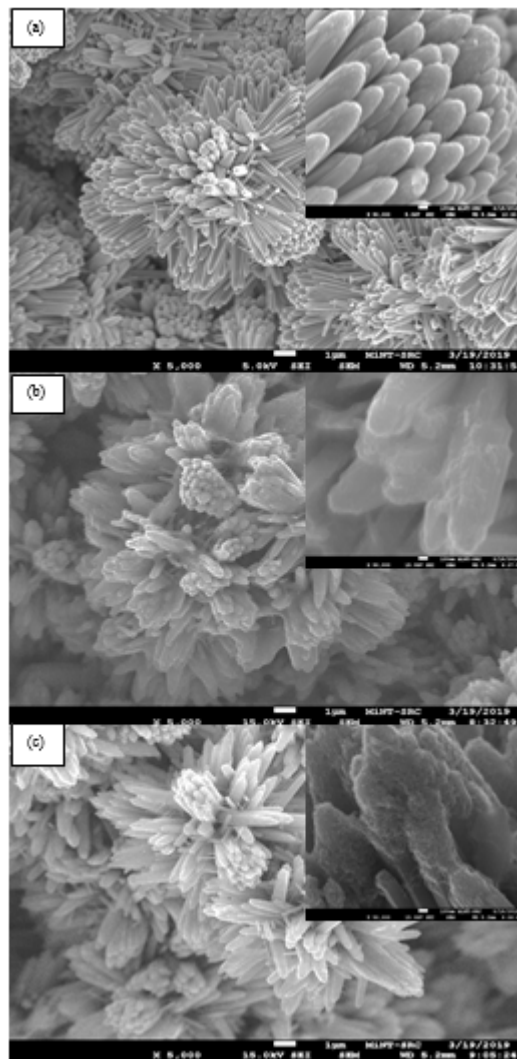


**Figure 4:** Surface morphology of (a) R-Ag/TiO<sub>2</sub> film and AR-Ag/TiO<sub>2</sub> film prepared at (b) 1 hour and (c) 2 hours

### 3.4 Photocatalytic analysis

The investigation of prepared sample towards MB degradation was conducted in order to find the efficiency. Figure 5 shows the decreasing initial absorbance of MB that disappeared almost completely after 90 minutes of irradiation at 664 nm wavelength. Figure 5(b) is the photolysis (absence of catalyst) experiment and was conducted to act as a reference. Figure 5(b)-(d) shows the absorbance result for R-Ag/TiO<sub>2</sub> and AR-Ag/TiO<sub>2</sub>. The result also shows the time dependent of light irradiation of the prepared samples. Figure 6 shows degradation rate of MB is plotted against time to



observe the photocatalytic efficiency for all samples. The direct photolysis shows 66% degradation, R-Ag/TiO<sub>2</sub> film shows 85%, AR1-Ag/TiO<sub>2</sub> film has 98% and AR2-Ag/TiO<sub>2</sub> film has 94%. This results exhibits the anatase phase play an important role in enhancing photodegradation of MB. For R-Ag/TiO<sub>2</sub> film also has high degradation. It proved that the single crystalline which is rutile phase can provide good mobility. Then, Ag metal play an important role in capturing electron that act as electron trap. This phenomenon also agreed with previous study [48]. The Schottky barrier that develop between TiO<sub>2</sub> and Ag metal enhance the electron lifetime and provide more time for electron and hole to react with the targeted contaminants [49]. Moreover, the addition of anatase nanoparticle that developed from the immersion of tayca 302 give a huge advantage by providing active surface site. The anatase phase also assisted to hold electron more after being capture from R-Ag/TiO<sub>2</sub> film.

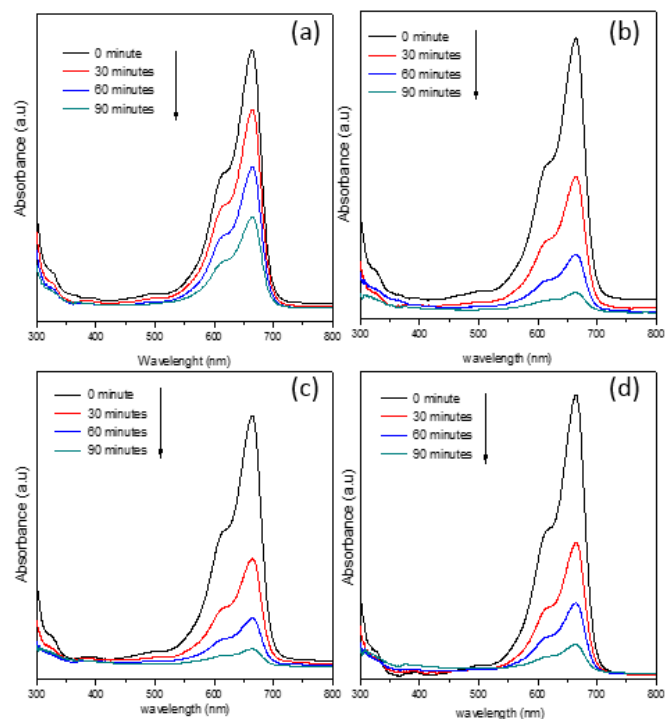
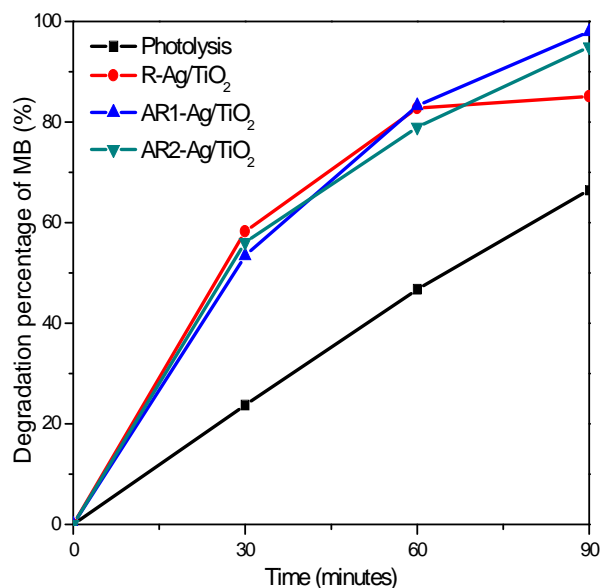


**Figure 5:** Photodegradation of MB for (a) photolysis (b) R-Ag/TiO<sub>2</sub> film and AR-Ag/TiO<sub>2</sub> film prepared at (c) 1 hour and (d) 2 hours

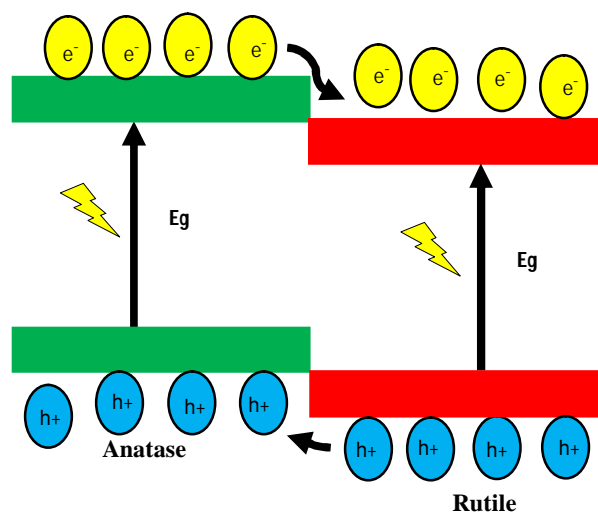
The 2 hours immersion shows the decreased in photodegradation which is only 94% degradation. This reduced result may be too much anatase nanoparticle decorated on the rods and act as the recombination centre. This phenomenon will lead to decrease the photocatalytic activity. In photocatalytic activity, several factors contribute to the high degradation such as crystallinity, surface morphology and surface chemistry [50], [51]. One of the important factor is lifetime electron that produce during the excitation. This will hold electron longer and help to electron and hole to react with the contaminants. Figure 7 shows the

illustration of electron flow between anatase and rutile phase.

The electron excited from valence band (VB) to the conduction band (CB) upon irradiation that has enough energy. The photogenerated electron flow from anatase phase to rutile phase while the photogenerated hole flow from the opposite site from rutile phase to anatase phase. This may due to the anatase/rutile heterojunction that exist in bi layer film or composite powder [52], [53]. This heterojunction inhibit the recombination between electron and hole. Subsequently, the electron was further trapped in Ag element and give more lifetime to the electron to react with the contaminants.



**Figure 6:** Degradation percentage for photolysis, R-Ag/TiO<sub>2</sub> film and AR-Ag/TiO<sub>2</sub> film prepared at 1 hour and 2 hours



**Figure 7:** The illustration of electron flow between anatase and rutile phase

## 5. CONCLUSION

Mixed anatase/rutile Ag doped titanium dioxide (TiO<sub>2</sub>) film was successfully fabricated by using two simple steps. This was done to determine the best layer build up anatase nanoparticle decorated on flowerlike Ag doped rutile in TiO<sub>2</sub> and to determine the best degradation rate. The XRD characterization showed the anatase phase peaks were able to be produce on rutile phase by the immersion immersion of tayca 320 solution. Furthermore, the characterization of FESEM showed the flowerlike structure growth on all samples and anatase particle decorated on top of the flowers. The EDX characterization proved there were no foreign elements beside TiO<sub>2</sub>. Finally, the photodegradation of AR-Ag/TiO<sub>2</sub> successfully shows the degradation rate of MB. The immersed sample was proven to show successful degradation rate as the methylene blue (MB) dye almost degraded completely in 90 minutes. The optimum immersion of 1 hours shows the best photodegradation and achieved 100 percent degradation in 90 minutes. In conclusion, this project has proven that the simple immersion method can produced mixed anatase/rutile Ag doped titanium dioxide (TiO<sub>2</sub>) film for enhance photocatalytic activity. The combination between mixed phase and Ag metal can provide more lifetime to the excited electron that act as electron trapped. Moreover, the decorated anatase also enhance the active surface site for photocatalytic activity take place. This film has a promising properties for waste water treatment for the industries.

## ACKNOWLEDGEMENT

The authors acknowledge the financial support given by the Research University Grant from Universiti Tun Hussein Onn (MDR Vot H471 and GPPS Vot U958). The author would also like to thank Center for Instrumental Analysis, Shizuoka University, Hamamatsu, Japan for the characterization equipment.

## REFERENCES

- [1] U. G. Akpan and B. H. Hameed, **Parameters affecting the photocatalytic degradation of dyes using TiO<sub>2</sub>-based photocatalysts: a review**, *Journal of hazardous materials*, vol. 170, no. 2–3, pp. 520–529, 2009.
- [2] N. H. H. Hairom, A. W. Mohammad, L. Y. Ng, and A. A. H. Kadhum, **Utilization of self-synthesized ZnO nanoparticles in MPR for industrial dye wastewater treatment using NF and UF membrane**, *Desalination and Water Treatment*, vol. 54, no. 4–5, pp. 944–955, 2015.
- [3] U. G. Akpan and B. H. Hameed, **Parameters affecting the photocatalytic degradation of dyes using TiO<sub>2</sub>-based photocatalysts: A review**, *Journal of Hazardous Materials*, vol. 170, no. 2–3, pp. 520–529, 2009.
- [4] S. Shoabargh, A. Karimi, G. Dehghan, and A. Khataee, **A hybrid photocatalytic and enzymatic process using glucose oxidase immobilized on TiO<sub>2</sub>/polyurethane for removal of a dye**, *Journal of Industrial and Engineering Chemistry*, vol. 20, no. 5, pp. 3150–3156, 2014.
- [5] M. A. Rauf and S. S. Ashraf, **Fundamental principles and application of heterogeneous photocatalytic degradation of dyes in solution**, *Chemical engineering journal*, vol. 151, no. 1–3, pp. 10–18, 2009.
- [6] K. H. Ng and C. K. Cheng, **A novel photomineralization of POME over UV-responsive TiO<sub>2</sub> photocatalyst: kinetics of POME degradation and gaseous product formations**, *RSC Advances*, vol. 5, no. 65, pp. 53100–53110, 2015.
- [7] H. Dong *et al.*, **An overview on limitations of TiO<sub>2</sub>-based particles for photocatalytic degradation of organic pollutants and the corresponding countermeasures**, *Water Research*, vol. 79. Elsevier Ltd, pp. 128–146, 2015.
- [8] J. H. Park, S. Kim, and A. J. Bard, **Novel carbon-doped TiO<sub>2</sub> nanotube arrays with high aspect ratios for efficient solar water splitting**, *Nano letters*, vol. 6, no. 1, pp. 24–28, 2006.
- [9] Y. Tao *et al.*, **Synthesis of Nanostructured TiO<sub>2</sub> Photocatalyst with Ultrasonication at Low Temperature**, *Journal of Materials Science and Chemical Engineering*, vol. 03, no. 01, pp. 29–36, 2015.
- [10] M. AHMAD, **Low temperature and normal pressure growth of rutile-phased TiO<sub>2</sub> nanorods/nanoflowers for DSC application prepared by hydrothermal method**, *Journal of Advanced Research in Physics*, vol. 3, no. 2, pp. 2011–2013, 2012.
- [11] X. H. Ning *et al.*, **Flower-shaped TiO<sub>2</sub> clusters for highly efficient photocatalysis**, *RSC Advances*, vol. 7, no. 55, pp. 34907–34911, 2017.
- [12] A. Primo, T. Marino, A. Corma, R. Molinari, and H. García, **Efficient visible-light photocatalytic water splitting by minute amounts of gold supported on nanoparticulate CeO<sub>2</sub> obtained by a biopolymer templating method**, *Journal of the American Chemical Society*, vol. 133, no. 18, pp. 6930–6933, 2011.
- [13] M. C. Wu *et al.*, **Nitrogen-doped anatase nanofibers decorated with noble metal nanoparticles for photocatalytic production of hydrogen**, *ACS Nano*, vol. 5, no. 6, pp. 5025–5030, 2011.
- [14] A. Folli, **TiO<sub>2</sub> photocatalysis in Portland cement systems: fundamentals of self cleaning effect and air pollution mitigation**, *University of Aberdeen, Scotland*, 2010.

- [15] F. H. Mustapha *et al.*, **New insight into self-modified surfaces with defect-rich rutile TiO<sub>2</sub> as a visible-light-driven photocatalyst**, *Journal of Cleaner Production*, vol. 168, pp. 1150–1162, 2017.
- [16] O. Diwald, T. L. Thompson, T. Zubkov, E. G. Goralski, S. D. Walck, and J. T. Yates, **Photochemical activity of nitrogen-doped rutile TiO<sub>2</sub>(110) in visible light**, *Journal of Physical Chemistry B*, vol. 108, no. 19, pp. 6004–6008, 2004.
- [17] J. Zhang, P. Zhou, J. Liu, and J. Yu, **New understanding of the difference of photocatalytic activity among anatase, rutile and brookite TiO<sub>2</sub>**, *Physical Chemistry Chemical Physics*, vol. 16, no. 38, pp. 20382–20386, 2014.
- [18] W. Zhao, C. Luan, X. Ma, X. Feng, L. He, and J. Ma, **Characterization of niobium-doped titania epitaxial films deposited by metalorganic chemical vapor deposition**, *Materials Characterization*, vol. 137, pp. 263–268, 2018.
- [19] T. A. Saleh and V. K. Gupta, **Photo-catalyzed degradation of hazardous dye methyl orange by use of a composite catalyst consisting of multi-walled carbon nanotubes and titanium dioxide**, *Journal of colloid and interface science*, vol. 371, no. 1, pp. 101–106, 2012.
- [20] A. Ramchiary and S. K. Samdarshi, **Ag deposited mixed phase titania visible light photocatalyst—Superiority of Ag-titania and mixed phase titania co-junction**, *Applied Surface Science*, vol. 305, pp. 33–39, 2014.
- [21] M. H. Mamat, M. Z. Sahdan, Z. Khusaimi, A. Z. Ahmed, S. Abdullah, and M. Rusop, **Influence of doping concentrations on the aluminum doped zinc oxide thin films properties for ultraviolet photoconductive sensor applications**, *Optical Materials*, vol. 32, no. 6, pp. 696–699, 2010.
- [22] R. A. Zayadi and F. A. Bakar, **Comparative study on the performance of Au/F-TiO<sub>2</sub> photocatalyst synthesized from Zamzam water and distilled water under blue light irradiation**, *Journal of Photochemistry and Photobiology A: Chemistry*, vol. 346, pp. 338–350, 2017.
- [23] L. G. Devi and R. Kavitha, **A review on plasmonic metal • TiO<sub>2</sub> composite for generation, trapping, storing and dynamic vectorial transfer of photogenerated electrons across the Schottky junction in a photocatalytic system**, *Applied surface science*, vol. 360, pp. 601–622, 2016.
- [24] A. Guillén-Santiago, S. A. Mayén, G. Torres-Delgado, R. Castaneda-Pérez, A. Maldonado, and M. de la L. Olvera, **Photocatalytic degradation of methylene blue using undoped and Ag-doped TiO<sub>2</sub> thin films deposited by a sol-gel process: Effect of the ageing time of the starting solution and the film thickness**, *Materials Science and Engineering: B*, vol. 174, no. 1–3, pp. 84–87, 2010.
- [25] M. Ahamed, M. A. M. Khan, M. J. Akhtar, H. A. Alhadlaq, and A. Alshamsan, **Ag-doping regulates the cytotoxicity of TiO<sub>2</sub> nanoparticles via oxidative stress in human cancer cells**, *Scientific Reports*, vol. 7, no. 1, pp. 1–14, 2017.
- [26] F. Paquin, J. Rivnay, A. Salleo, N. Stingelin, and C. Silva, **Multi-phase semicrystalline microstructures drive exciton dissociation in neat plastic semiconductors**, *J. Mater. Chem. C*, vol. 3, no. 207890, pp. 10715–10722, 2015.
- [27] V. Madhavi, P. Kondaiah, and M. R. G., **Influence of silver nanoparticles on titanium oxide and nitrogen doped titanium oxide thin films for sun light photocatalysis**, *Applied Surface Science*, vol. 436, pp. 708–719, 2018.
- [28] I. J. Gomez, B. Arnaiz, M. Cacioppo, F. Arcudi, and M. Prato, **Nitrogen-doped Carbon Nanodots for bioimaging and delivery of paclitaxel**, *Journal of Materials Chemistry B*, vol. 6, no. 35, pp. 7634–7639, 2018.
- [29] M. Pelaez *et al.*, **A review on the visible light active titanium dioxide photocatalysts for environmental applications**, *Applied Catalysis B: Environmental*, vol. 125, pp. 331–349, 2012.
- [30] S. Demirci, T. Dikici, M. Yurddaskal, S. Gultekin, M. Toparli, and E. Celik, **Synthesis and characterization of Ag doped TiO<sub>2</sub> heterojunction films and their photocatalytic performances**, *Applied Surface Science*, vol. 390, pp. 591–601, 2016.
- [31] S. C. Padmanabhan *et al.*, **A simple sol - Gel processing for the development of high-temperature stable photoactive anatase titania**, *Chemistry of Materials*, vol. 19, no. 18, pp. 4474–4481, 2007.
- [32] S. Perumal, K. MonikandaPrabu, C. G. Sambandam, and A. P. Mohamed, **Synthesis and characterization studies of solvothermally synthesized undoped and Ag-doped TiO<sub>2</sub> nanoparticles using toluene as a solvent**, *Journal of Engineering Research and Applications*, vol. 4, no. 7, pp. 184–187, 2014.
- [33] M. Kang, **The superhydrophilicity of Al-TiO<sub>2</sub> nanometer sized material synthesized using a solvothermal method**, *Materials Letters*, vol. 59, no. 24–25, pp. 3122–3127, 2005.
- [34] P. Chen, **A novel synthesis of Ti<sup>3+</sup> self-doped Ag<sub>2</sub>O/TiO<sub>2</sub> (p-n) nanoheterojunctions for enhanced visible photocatalytic activity**, *Materials Letters*, vol. 163, pp. 130–133, 2016.
- [35] J. Yu and J. C. Yu, **Photocatalytic Activity and Characterization of the Sol-Gel Derived Pb-Doped TiO<sub>2</sub> Thin Films**, *Journal of Sol-Gel Science and Technology*, pp. 39–48, 2002.
- [36] A. Fujishima, T. N. Rao, and D. A. Tryk, **Titanium dioxide photocatalysis**, *Journal of photochemistry and photobiology C: Photochemistry reviews*, vol. 1, no. 1, pp. 1–21, 2000.

- [37] J. Xu, Y. Ao, D. Fu, and C. Yuan, **Low-temperature preparation of F-doped TiO<sub>2</sub> film and its photocatalytic activity under solar light**, *Applied Surface Science*, vol. 254, no. 10, pp. 3033–3038, 2008.
- [38] S. DB and J. SK, **Time Dependent Facile Hydrothermal Synthesis of TiO<sub>2</sub> Nanorods and their Photoelectrochemical Applications**, *Journal of Nanomedicine & Nanotechnology*, vol. 01, no. s7, 2015.
- [39] N. K. A. Hamed, N. S. Khalid, F. I. Mohd Fazli, M. L. Mohd Napi, N. Nayan, and M. K. Ahmad, **Influence of hydrochloric acid volume on the growth of titanium dioxide (TiO<sub>2</sub>) nanostructures by hydrothermal method**, *Sains Malaysiana*, vol. 45, no. 11, pp. 1669–1673, 2016.
- [40] Z. He *et al.*, **Photocatalytic activity of TiO<sub>2</sub> containing anatase nanoparticles and rutile nanoflower structure consisting of nanorods**, *Journal of Environmental Sciences*, vol. 25, no. 12, pp. 2460–2468, 2013.
- [41] S. A. Abdullah *et al.*, **Influence of substrate annealing on inducing Ti 3+ and oxygen vacancy in TiO<sub>2</sub> thin films deposited via RF magnetron sputtering**, *Applied Surface Science*, vol. 462, pp. 575–582, 2018.
- [42] T. Dhandayuthapani, R. Sivakumar, and R. Ilangovan, **Growth of micro flower rutile TiO<sub>2</sub> films by chemical bath deposition technique: Study on the properties of structural, surface morphological, vibrational, optical and compositional**, *Surfaces and Interfaces*, vol. 4, pp. 59–68, 2016.
- [43] M. Ye, H. Y. Liu, C. Lin, and Z. Lin, **Hierarchical rutile TiO<sub>2</sub> flower cluster-based high efficiency dye-sensitized solar cells via direct hydrothermal growth on conducting substrates**, *Small*, vol. 9, no. 2, pp. 312–321, Jan. 2013.
- [44] X. Meng *et al.*, **Formation mechanism of rutile TiO<sub>2</sub> rods on fluorine doped tin oxide glass**, *Journal of Nanoscience and Nanotechnology*, vol. 14, no. 11, pp. 8839–8844, 2014.
- [45] R. V Nair, M. Jijith, V. S. Gummaluri, and C. Vijayan, **A novel and efficient surfactant-free synthesis of Rutile TiO<sub>2</sub> microflowers with enhanced photocatalytic activity**, *Optical Materials*, vol. 55, pp. 38–43, 2016.
- [46] S. Malali and M. Foroutan, **Dissociation behavior of water molecules on defect-free and defective rutile TiO<sub>2</sub> (1 0 1) surfaces**, *Applied Surface Science*, vol. 457, pp. 295–302, 2018.
- [47] I. M. Arabatzis *et al.*, **Preparation, characterization and photocatalytic activity of nanocrystalline thin film TiO<sub>2</sub> catalysts towards 3,5-dichlorophenol degradation**, *Journal of Photochemistry and Photobiology A: Chemistry*, vol. 149, no. 1–3, pp. 237–245, 2002.
- [48] B. A. Akgun, A. W. Wren, C. Durucan, M. R. Towler, and N. P. Mellott, **Sol-gel derived silver-incorporated titania thin films on glass: bactericidal and photocatalytic activity**, *Journal of sol-gel science and technology*, vol. 59, no. 2, pp. 228–238, 2011.
- [49] C. Peng, W. Wang, W. Zhang, Y. Liang, and L. Zhuo, **Surface plasmon-driven photoelectrochemical water splitting of TiO<sub>2</sub> nanowires decorated with Ag nanoparticles under visible light illumination**, *Applied Surface Science*, vol. 420, pp. 286–295, 2017.
- [50] M. Y. Ghaly, T. S. Jamil, I. E. El-Seesy, E. R. Souaya, and R. A. Nasr, **Treatment of highly polluted paper mill wastewater by solar photocatalytic oxidation with synthesized nano TiO<sub>2</sub>**, *Chemical Engineering Journal*, vol. 168, no. 1, pp. 446–454, 2011.
- [51] E. Bae, N. Murakami, and T. Ohno, **Exposed crystal surface-controlled TiO<sub>2</sub> nanorods having rutile phase from TiCl<sub>3</sub> under hydrothermal conditions**, *Journal of Molecular Catalysis A: Chemical*, vol. 300, no. 1–2, pp. 72–79, 2009.
- [52] C. Wang *et al.*, **Rutile TiO<sub>2</sub> nanowires on anatase TiO<sub>2</sub> nanofibers: a branched heterostructured photocatalysts via interface-assisted fabrication approach**, *Journal of colloid and interface science*, vol. 363, no. 1, pp. 157–164, 2011.
- [53] Y. Yamada and Y. Kanemitsu, **Blue photoluminescence of highly photoexcited rutile TiO<sub>2</sub>: Nearly degenerate conduction-band effects**, *Physical Review B - Condensed Matter and Materials Physics*, vol. 82, no. 11, pp. 1–4, 2010.